

Which Modality should I use - Text, Motif, or Image? : Understanding Graphs with Large Language Models

Debarati Das Ishaan Gupta Jaideep Srivastava Dongyeop Kang

Department of Computer Science, University of Minnesota
{das00015, gupta737, srivasta, dongyeop}@umn.edu

Abstract

Large language models (LLMs) are revolutionizing various fields by leveraging large text corpora for context-aware intelligence. Due to the context size, however, encoding an entire graph with LLMs is fundamentally limited. This paper explores how to integrate graph data with LLMs better and presents a novel approach using various encoding modalities (e.g., text, image, and motif) and approximation of global connectivity of a graph using different prompting methods to enhance LLMs' effectiveness in handling complex graph structures. The study also introduces GRAPHTMI, a new benchmark for evaluating LLMs in graph structure analysis, focusing on factors such as homophily, motif presence, and graph difficulty. Key findings reveal that image modality, supported by advanced vision-language models like GPT-4V, is more effective than text in managing token limits while retaining critical information. The research also examines the influence of different factors on each encoding modality's performance. This study highlights the current limitations and charts future directions for LLMs in graph understanding and reasoning tasks.

1 Introduction

Large Language Models (LLMs) have expanded their utility beyond traditional language processing, becoming increasingly valuable in robotics, planning, and reasoning (Huang and Chang, 2022; Andreas, 2022; Madaan et al., 2022). Their versatility has extended to domains with inherent graph structures, such as social network analysis (Mislove et al., 2007), drug discovery (Vishveshvara et al., 2002), and recommendation systems (Melville and Sindhvani, 2010). However, despite their success, LLMs are hindered by a dependence on unstructured text, leading to issues like hallucination or logical oversights (Zhang et al., 2023). This limitation and the challenge of incorporating new, post-training data (Lewis et al., 2020) about

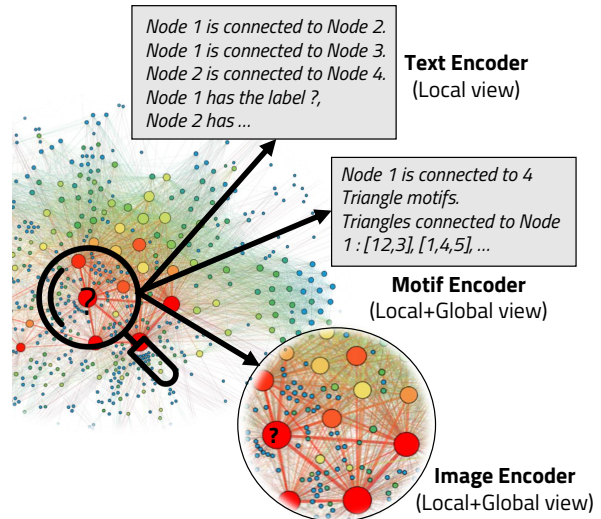


Figure 1: Input modality encoding for graphs impacts node classification, with text modality offering detailed information from a local point of view but violating the input context limitations for LLMs due to verbosity. Motif encoding provides local and global context, while image modality gives a comprehensive global view, efficiently processed by GPT-4V, which integrates capabilities from both vision and text.

the world's changing state can be addressed using graph-structured external data (Pan et al., 2023).

While strides have been made in interpreting multi-modal information (Yin et al., 2023), integrating graph understanding in LLMs is still an emerging exploration. Specifically, LLMs need help to handle complex graph-structured data that cannot be directly ingested as an input. Therefore, designing an efficient input encoding and appropriate prompts for different graph tasks is an interesting problem explored by recent papers (Fatemi et al., 2023; Chen et al., 2023). However, these papers use a constrained experimental setup, where the real-world graph size is either limited by heuristic constraints (e.g., number of nodes) (Guo et al., 2023) or synthetic graphs are constructed (Wang et al., 2023) to verify their experiments. Real-world

graphs are too large to be fed as input because of the context window limitations of LLMs. This research gap motivates us to think about other possible encoding modalities or approximation methods that can provide graphs as input to LLMs.

In this paper, we explore the impact of encoding global and local graph structures using different modalities, particularly focusing on node classification tasks. In specific, we compare three modalities: *Text*, *Motif*, and *Image* (See Figure 1). Text modality encoding provides a detailed local perspective of the subgraph and its connections. However, it becomes too verbose for large graphs, potentially exceeding the input context limits of large language models like GPT-4 (Bubeck et al., 2023). To circumvent this, we suggest Motif modality encoding, which captures essential patterns within the node’s vicinity, offering a balanced local and global perspective. Finally, we propose image modality encoding as an alternative, potentially superior to text, due to its ability to convey a more global view of the node’s neighborhood with fewer tokens, making efficient use of the input context. GPT-4V (OpenAI, 2023a), a recently released, vision-capable iteration of GPT-4, facilitates this approach. We evaluate all three encoding modalities for the task of node classification using a combination of four metrics (accuracy rate, mismatch rate, denial rate, and token limit fraction), which together capture the tradeoff between an informative yet not verbose prompt.

Main contributions:

- We conduct a comprehensive breadth-first analysis of graph-structure prompting in different modalities, including text, image, and motif, using large language and vision-language models for node classification tasks.
- We also conduct a depth-first analysis of how different factors influence the performance of each encoding modality.
- We introduce GRAPHTMI, a novel graph benchmark featuring a hierarchy of graphs, associated prompts, and encoding modalities designed to further the community’s understanding of graph structure effects using LLMs.

Some key findings: 1) The image modality is better suited than the text modality for graphs when the need is to balance a token limit constraint while retaining important information. 2) Graph task dif-

ficulty based on homophily and motif counts is a factor in deciding which encoding modality to use for classification. 3) Factors like edge encoding function, graph structure, and graph sampling techniques impact the performance of node classification using text modality. 4) Motif attachment information has a more significant impact on node classification than motif count information. 5) Improving image representation impacts the performance of node classification using image modality.

Our empirical results show that, while LLMs are getting better at handling graph data, they still have to improve to catch up with GNN models that work with real-world graphs. Through our study, we uncover current limitations and future directions of LLMs equipped with image understanding in comprehending graphs and performing associated reasoning tasks.

2 Proposed Methods

Graph encoding is necessary for turning graph-structured information into a sequence for consumption by language models. Figure 2 describes our experiment setup, where the modality encoder inputs the graph structure and a graph query (for node classification, the query would be “Predict the label of the node marked with ?”). Depending on the modality chosen (for text and motif modality, we choose GPT-4; for image modality, we choose GPT-4V), we encode the graph structure appropriately and pass it as a prompt to the LLM, generating the desired label.

2.1 Text Encoding Modality

Encoding graphs as text can be separated into two key parts: First, the mapping of nodes to their corresponding labels in the graph, and second, the encoding of edges between the nodes. We encode the node-to-label mapping as a dictionary of type {node ID: node label}. Edge encoding representations have been explored in recent works (Guo et al., 2023; Fatemi et al., 2023). Text encodings of graphs provide the LLM, GPT-4 (OpenAI, 2023a), with the local context of the labeled node in the form of individual edge connections and node label information. As the size of the graph increases, these text encodings can get quite verbose, add to confusion, and violate the input context window of the LLMs. Therefore, finding a suitable, informative, yet compressed representation of the graph structure or edge representation becomes impera-

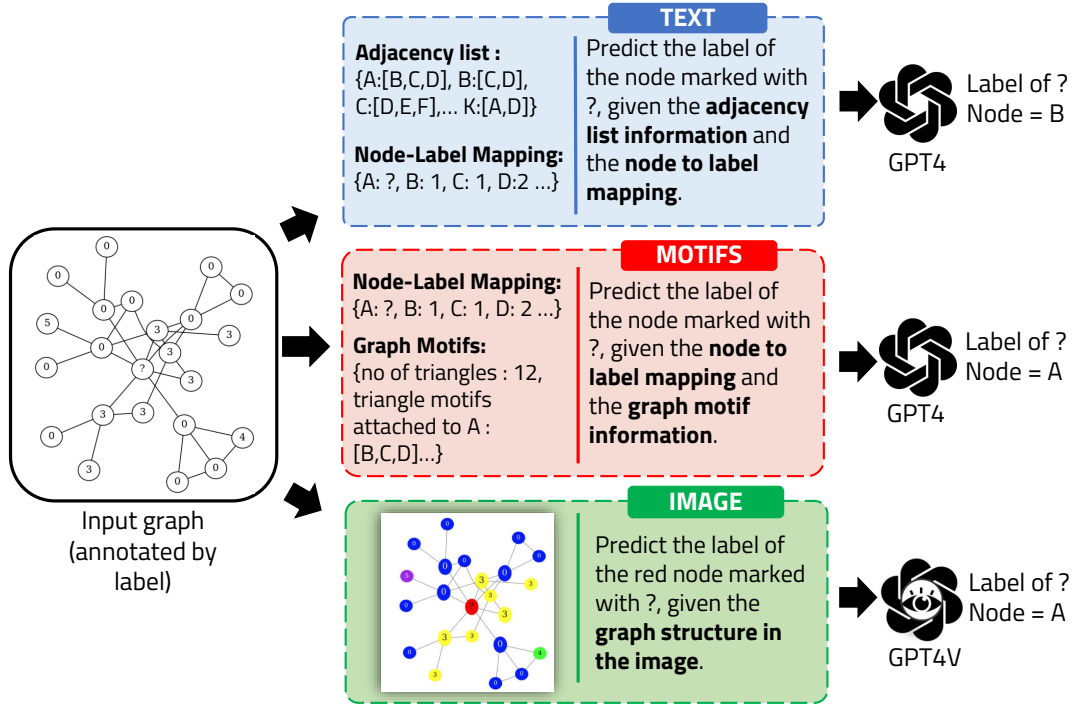


Figure 2: Node Classification on a Graph using different input modality encodings like Text, Motif, and Image.

tive. We consider the importance of some factors that can influence the performance of text modality encoding:

Edge Encoding Function: Motivated by recent works (Fatemi et al., 2023; Guo et al., 2023) describing the importance of selecting the appropriate text encoding for a graph, we experiment with different edge representations on real-world datasets and evaluate the metrics for node classification.

Graph Structure: Recent work (Yasir et al., 2023; Palowitch et al., 2022) explores the impact of graph structure on graph reasoning tasks. We selected real-world citation datasets with differing network properties to explore the significance of graph structure on node classification.

Sampling Strategy: Graph sampling methods are crucial for graph reasoning with Large Language Models (LLMs) due to context window limitations and the complex nature of real-world graphs (Wei and Hu, 2022). Two methods, Ego graph (Stolz and Schlereth, 2021) and Forest Fire sampling (Leskovec and Faloutsos, 2006), offer distinct perspectives. Ego graph sampling focuses on a central node and its immediate neighbors, creating a subgraph that reflects their connections. On the other hand, Forest Fire sampling starts from a random node and expands outwards, resulting in subgraphs that vary in size and local structure, influenced by

parameters like burning probabilities.

An example prompt generated after applying the text encoding modality looks like:

```

Task: Node Label Prediction (Predict the label of the node marked with a ?) given the adjacency list information as a dictionary of type "node: neighborhood" and node-label mapping in the text enclosed in triple backticks. Response should be in the format "Label of Node = <predicted label>". If the predicted label cannot be determined, return "Label of Node = -1".
```AdjList: {1: [2,3], 2: [3,4], 3: [1,2]}
Node-Label Mapping: {1: A, 2: B, 3: ?}```

```

## 2.2 Motif Modality

In networks, significant repeating patterns, or “motifs”, act as functional building blocks, revealing local structures and group behaviors in social and biological networks (Milo et al., 2002; Carrington et al., 2005; Holland and Leinhardt, 1974). The intuition behind the motif modality encoding is to provide the LLM with a local and global context of the graph structure by giving it, as input, the significant patterns around the vicinity of the unlabeled node, which could aid in its classification (Yang et al., 2018).

Encoding graphs as motifs can be separated into two key parts: First, the encoding of nodes to their corresponding labels in the graph, and second, the motifs present around the ? (unlabeled) node. We

encode the node-to-label mapping as a dictionary of type {node ID: node label}. we calculate motifs in the neighborhood of the ? nodes and pass this information to GPT-4 (OpenAI, 2023a) as the graph-motif information. We consider the importance of different network motifs, such as the count and presence of star motifs, triangle motifs, and clique information (Felmlee et al., 2021) that can influence the performance of the motif modality encoding.

An example prompt generated after applying the motif encoding modality looks like:

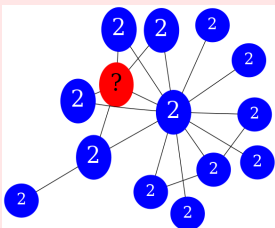
**Task:** Node Label Prediction (Predict the label of the node marked with a ?) given the node-label mapping and graph motif information in the text enclosed in triple backticks. Response should be in the format "Label of Node = <predicted label>". If the predicted label cannot be determined, return "Label of Node = -1".  
 ```Node-Label Mapping: {1: A, 2: A, 3: ?}  
 Graph-motif information: No of triangles: 1| Triangles attached to ? Node : [1,2,3]```\`

2.3 Image Modality

This modality is inspired by the saying that "a picture is worth a thousand words." Images, offering a rich and complex data representation, can convey intricate structures more efficiently than text. They can express complex networks, labels, spatial relationships, and non-verbal cues (like visually emphasizing key nodes) in fewer tokens than images. We use VLMs like GPT-4V (OpenAI, 2023b) to process graph images to give LLMs a global perspective of graph structural information. GPT-4V, a multimodal model, interprets various visuals by leveraging its language skills. Enhancing a graph's image representation is crucial for improving its node classification performance in the image modality.

An example prompt generated after applying the image encoding modality looks like this:

Task: Node Label Prediction (Predict the label of the red node marked with a ?, given the **graph structure information in the image**). Response should be in the format "Label of Node = <predicted label>". If the predicted label cannot be determined, return "Label of Node = -1"



3 Data and Experimental Setup

3.1 Seed Datasets

We experiment with three citation network datasets, which are popular node classification benchmarks, CORA (McCallum et al., 2000) with seven categories : [0-Rule Learning, 1-Neural Networks, 2-Case-Based, 3-Genetic Algorithms, 4-Theory, 5-Reinforcement Learning, and 6-Probabilistic Methods], CITESEER (Giles et al., 1998) with six categories of areas in Computer Science: [0-Agents, 1-ML, 2-IR, 3-DB, 4-HCI, 5-AI] and PUBMED (Sen et al., 2008) that consists of scientific journals collected from the PubMed database with the following three categories: [0-Diabetes Mellitus, Experimental, 1-Diabetes Mellitus Type 1, 2-Diabetes Mellitus Type 2]. In this paper, we are only interested in the structural information of the graph toward node classification. Therefore, we utilize only node and label IDs for our experiments.

3.2 Evaluation Metrics

This paper uses four metrics to evaluate the performance of the downstream task of node classification.

Accuracy Rate A : This metric indicates the LLM's performance on the task of node classification.

$$A = \frac{\text{No. of correct predictions}}{\text{Total no. of samples}} \quad (1)$$

Mismatch Rate M : This metric indicates the degree of misclassification by LLM (when the ground truth value is not the same as the predicted value).

$$M = \frac{\text{No. of incorrect predictions}}{\text{Total no. of samples}} \quad (2)$$

Denial Rate D : When we craft our prompt, we instruct the LLM to return -1 if it cannot predict the label of the ? node (node to be classified). The denial rate metric describes the rate of failure of the LLM (when the predicted value is -1).

$$D = \frac{\text{No. of predictions} = -1}{\text{Total no. of samples}} \quad (3)$$

$$1 - A = M + D \quad (4)$$

Token Limit Fraction T : This metric measures how the encoding modality of an LLM utilizes its input context window, assessing the impact of token constraints linked to the model's neural network architecture. In transformer-based models

like GPT-3, GPT-4, and GPT-4V, a fixed-size attention window limits the number of tokens processed simultaneously, affecting computational cost and performance.

$$T = \frac{\text{Number of usage tokens}}{\text{Token limit constraint for the model}} \quad (5)$$

We use these four metrics in combination to evaluate node classification using different encoding modalities because we are trying to capture the tradeoff between informativeness and verbosity of the encoding. Metrics like accuracy(\uparrow), denial (\downarrow), and mismatch (\downarrow) capture the informativeness of the prompt, while the token limit fraction (\downarrow) captures the verbosity of the prompt. In the brackets, we denote the desired trend from each metric.

3.3 Graph Encoder Baselines

We compare our LLM models, which use different encoding modalities, to traditional graph learning models GCN(Kipf and Welling, 2016), GRAPH-SAGE(Hamilton et al., 2017) and GAT (Veličković et al., 2017) as a baseline for node classification tasks. We provide the training details for each GNN model in Appendix A.

3.4 Text Modality Setup

We explore multiple factors that could impact node classification in the text modality setup, such as the edge encoding function used, underlying graph structure, and graph sampling methods.

Impact of Edge encoding function: (Fatemi et al., 2023) describe the significant impact of graph encoding function on the performance of LLMs on graph-related tasks on simulated graphs. Motivated by this work, we experiment with different edge representations, shown in Table 2, on real-world datasets and evaluate the metrics for node classification.

Impact of Graph Structure : We selected real-world citation datasets (mentioned in section 3.1) with differing network properties to explore the significance of graph structure on node classification. Table 1 describes the difference between these datasets’ network properties. The definitions for these properties are provided in the Appendix B. Table 1 shows that Pubmed is the largest and most connected network, with a single connected component and a higher average degree. However, it has the lowest clustering coefficient, suggesting less local clustering among its nodes. Citeseer, while larger than CORA in terms of nodes, is the

| Properties | CORA | Citeseer | Pubmed |
|-------------|----------|----------|--------|
| Classes | 7 | 6 | 3 |
| Nodes | 2,708 | 3,327 | 19,717 |
| Edges | 5,278 | 4,552 | 44,324 |
| Density | 0.0014 | 0.0008 | 0.0002 |
| Avg deg | 3.89 | 2.74 | 4.49 |
| Clust coeff | 0.24 | 0.14 | 0.06 |
| Diameter | ∞ | ∞ | 18 |
| Components | 78 | 438 | 1 |
| 2-hop nodes | 36 | 15 | 60 |

Table 1: Comparison of network properties of popular citation network datasets CORA, Citeseer and Pubmed.

most fragmented, with many disconnected components and the lowest density. CORA has the highest density and clustering coefficient despite being the smallest network, indicating more local connectivity.

Impact of Sampling Strategy: We experiment with two distinct graph sampling strategies to understand the impact on node classification. We expect that while Forest Fire sampling tends to provide a more representative view of the entire network, particularly in large, single-component networks (Pubmed), Ego graph sampling excels in analyzing local community structures around specific nodes, proving more effective in networks where local structures are interesting (CORA, Citeseer). Both methods, however, can skew perceptions of a network’s overall structure, especially in diverse and expansive networks.

3.5 Motif Modality Setup

We experiment with different network motifs as input to the modality encoder. Table 3 describes the different types of motifs considered, a description of the motif, and an example of the encoding generated as input to GPT-4. Implementation details are in the Appendix.

We distinguish between providing the count of motifs in a graph and the members of the motifs attached to the unlabeled node. We hypothesize that if the unlabeled node is connected to an influential node (star motif) or an influential community of nodes (triangle or clique), it could influence the node’s label much more than the motif count (Tu et al., 2018) information, which merely provides the frequency of a motif in the provided graph. Similarly, when a node is the center of a star motif, it implies that it is an influential node with many

| Edge Representation | Text Encoding | Description of Edge Representation |
|-----------------------|--|--|
| Edgelist | Node to Label Mapping : Node 69025: Label 34 Node 17585: Label 10 ...
Edge list: [(69025, 96211), (69025, 17585), (17585, 104598), (17585, 18844), (17585, 96211), (96211, 34515)] | An Edgelist is a graph data structure that represents a graph by listing the edge connections between two nodes. (A, B) indicates a connection between nodes A and B. |
| Edgetext | Node to Label Mapping : Node 85328: Label 16 Node 158122: Label ? ...
Edge connections (source node - target node): Node 85328 is connected to Node 158122. Node 158122 is connected to Node 167226. | An Edgetext explicitly lists the connections between two nodes; for example, Node A is connected to Node B or Node A - Node B |
| Adjacency List | Node to Label Mapping : Node 2339: Label 3 Node 2340: Label ? ...
Adjacency list: 1558: [2339, 2340], 2339: [1558, 2340], 2340: [2339, 1558] | An adjacency list represents a graph as an array of linked lists. The index of the array represents a vertex, and each element in its linked list represents the other vertices that form an edge with the vertex. For example, A: [B, C] shows that A is connected to B and C. This gives an idea of node-neighborhood |
| GML | GraphML: graph [
node [
id 2339
label 3
]
node [
id 2340
label ?
]
node [
id 1558
label 3
]
edge [
source 2339
target 1558
]
edge [
source 2339
target 2340
]
] | A GraphML format consists of an unordered sequence of node and edge elements enclosed within []. Each node element has a distinct id and label attribute contained within []. Each edge element has source and target attributes contained within [] that identify the endpoints of an edge by having the same value as the node id attributes of those endpoints. The node label information is embedded within the structure, meaning no node-label mapping is notneeded. |
| GraphML | GraphML: <graphml xmlns=http://graphml.graphdrawing.org/xmlns xmlns:xsi=http://www.w3.org/2001/XMLSchema-instance xsi:schemaLocation=http://graphml.graphdrawing.org/xmlns http://graphml.graphdrawing.org/xmlns/1.0/graphml.xsd> <graph edgedefault=undirected>
<node id=2339 label=3 />
<node id=2340 label=? />
<node id=1558 label=3 />
<edge source=2339 target=1558 />
<edge source=2339 target=2340 />
</graph>
</graphml> | A GraphML file consists of an XML file containing a graph element, within which is an unordered sequence of node and edge elements. Each node element should have a distinct id attribute as well as its label, and each edge element has source and target attributes that identify the endpoints of an edge by having the same value as the id attributes of those endpoints. The node label information is embedded within the structure meaning no node-label mapping is needed. |

Table 2: Summary of edge representation passed as a part of the text modality encoder with their associated examples and explanations. We find that the **Adjacency list** representation provides a granular yet not too verbose view of the graph being passed to the LLM.

nodes citing it (in a citation network). When a node is part of a triangle motif or a bigger clique, it means that the node is part of a tightly-knit community of highly connected nodes, therefore, all the neighboring node labels influence the node’s label.

3.6 Image Modality Setup

Using the image modality, we experiment with multiple ways to represent the graph structure. We first generate the graph rendering of our sampled graphs using NetworkX (Hagberg et al., 2008) and color the nodes per the label values of each node. We set the unlabeled node always to be “red” and have a ? mark as a label on the node. No other node except the unlabeled node can be red. We intend to implicitly convey to the VLM (GPT-4V) that

the node classification should be based on the label corresponding to the node’s coloring. We then observe that the classification performance could still use improvement and hypothesize that the improvement could be a function of some image representation changes. Figure 3 illustrates how applying different changes to the image representation can enhance an image’s human readability. We then use these image encodings to evaluate the performance of node classification.

3.7 Creating the GraphTMI Benchmark

We identify that not all graphs are equally easy for node classification with all modalities. Depending on the “difficulty” of the graph, a particular encoding modality (or combinations) might be bet-

| Type of Motif | Motif Encoding | Description of Motif |
|--|--|---|
| Node-Label Mapping | Node to Label Mapping : Node 1889: Label 4 ... Node 1893: Label ?!... | Only the node-label mapping is provided (this gives no connectivity information to LLM) |
| No. of Star Motifs | Node to Label Mapping : Node 1889: Label 4 ... Node 1893: Label ?! ... Graph motif information: Number of star motifs: 0! | Star motifs signify centralized networks with influential central nodes, where a central node is connected to others that aren't interlinked. We pass the count of the star motifs present in the graph. |
| No. of Triangle Motifs | Node to Label Mapping : Node 1889: Label 4 ... Node 1893: Label ?! ... Graph motif information: Number of triangle motifs: 6! | Triangle motifs (triads connecting three nodes) are foundational in social networks, indicating transitive relationships, community structures, and strong social ties. We pass the count of the triads present in the graph. |
| No. of Triangle Motifs Attached | Node to Label Mapping : Node 1889: Label 4 ... Node 1893: Label ?!... Graph motif information: Triangle motifs attached to ? node: [1893,2034,1531], [1893,1531,429] | We pass the triangle motifs attached to the ? label, which gives an idea of the influential triads connected to the ? node. |
| No. of Star Motifs Attached | Node to Label Mapping : Node 1889: Label 4 ... Node 1893: Label ?!... Graph motif information: Star motifs connected to ? node: [] | We pass the star motifs attached to the ? label, which gives an idea of the influential nodes connected to the ? node. |
| No. of Star and Triangle Motifs | Node to Label Mapping : Node 1889: Label 4 ... Node 1893: Label ?!... Graph motif information: Number of star motifs: 0! Number of triangle motifs: 6! | We pass the count of the triads and star motifs present in the graph, to give the LLM an idea of the graph structure. |
| Star and Triangle Motifs attached | Node to Label Mapping : Node 1889: Label 4 ... Node 1893: Label ?!... Graph motif information: Triangle motifs attached to ? node: [1893,2034,1531], [1893,1531,429] Star motifs connected to ? node: [] | We pass the star motifs and triads attached to the ? label, which gives an idea of the influential nodes and triads connected to the ? node. |
| No of cliques ? Node is part of | Node to Label Mapping : Node 1889: Label 4 ... Node 1893: Label ?!... Graph motif information: Number of cliques in graph: 0! ? Node is a part of these cliques: [] | We pass the number of cliques in the network, which gives an idea of its clustered nature. We also pass the cliques the ? label is a part of, which gives an idea of the immediate community of the unlabelled node. |
| No of cliques ? Node is attached to | Node to Label Mapping : Node 1889: Label 4 ... Node 1893: Label ?!...Graph motif information: ? Node is attached to these cliques: [] | We pass the cliques the ? label is attached to, which gives an idea of the neighboring influential community of the unlabelled node. |

Table 3: Summary of motif information passed as a part of the motif modality encoder with their associated examples and explanations. The **Aggregate of all changes** setup combines all of the above motif information to give the LLM a local and global view of the graph being passed.

ter suited. We decide on graph “difficulty” based on the dual criteria of 1) count of motifs and 2) homophily in the graph.

The intuition behind the homophily criteria, in network theory (McPherson et al., 2001), is that nodes are likely to form connections with similar nodes rather than dissimilar ones. Thus, a graph that has a higher degree of homophily (multiple same labels present in the graph) would be much easier to classify as compared to a graph with a higher degree of heterophily (multiple different labels present in the graph), as the unlabeled node can be predicted based on the similar labels of its neighbors. This is illustrated in Figure 4, which shows examples from the CORA dataset (7 labels). Here, we see that the label of the red node in (a) is much easier to infer than (b) or (c). We apply a naive heuristic to decide homophily, i.e., the count of the distinct labels in the graph. If the count of distinct labels < 3 , the graph is considered *easy*. If the count is ≥ 3 and < 5 , it is considered *medium*, and if the count is ≥ 5 , it is considered *hard*.

The intuition behind the count of motifs criteria is that a graph with multiple network motifs

is more complex (Tu et al., 2018) and, therefore, more difficult to classify. We see this in Figure 4, where graphs (b) and (c) have multiple kinds of motifs, and it is more difficult to infer the label of the red node. To decide the motif criteria, we count the total number of motifs (focusing on just triads, star motifs, and cliques) in a graph. For example, if this count of motifs ≤ 10 for the CORA dataset, the graph is considered *easy*. If the count is > 10 and ≤ 20 , it is regarded as *medium*; if the count is > 20 , it is considered *hard*. Some graphs can have both the homophily and motif criteria applicable to them; for instance, Figure 4 (b) can be classified as *medium* based on homophily, *hard* based on the count of motifs. This leads us to combine the homophily and the count of motif criteria to define the “task difficulty”. Thus, we can have $2^3 = 8$ categories of difficulty, and the final difficulty label is decided by choosing the higher annotation between homophily and count of motif classification). So, a graph with criteria {easy, hard} will be assigned the final task difficulty, *hard*.

Thus, we can classify graphs based on our “task difficulty” heuristic, and we introduce GRAPH-TMI

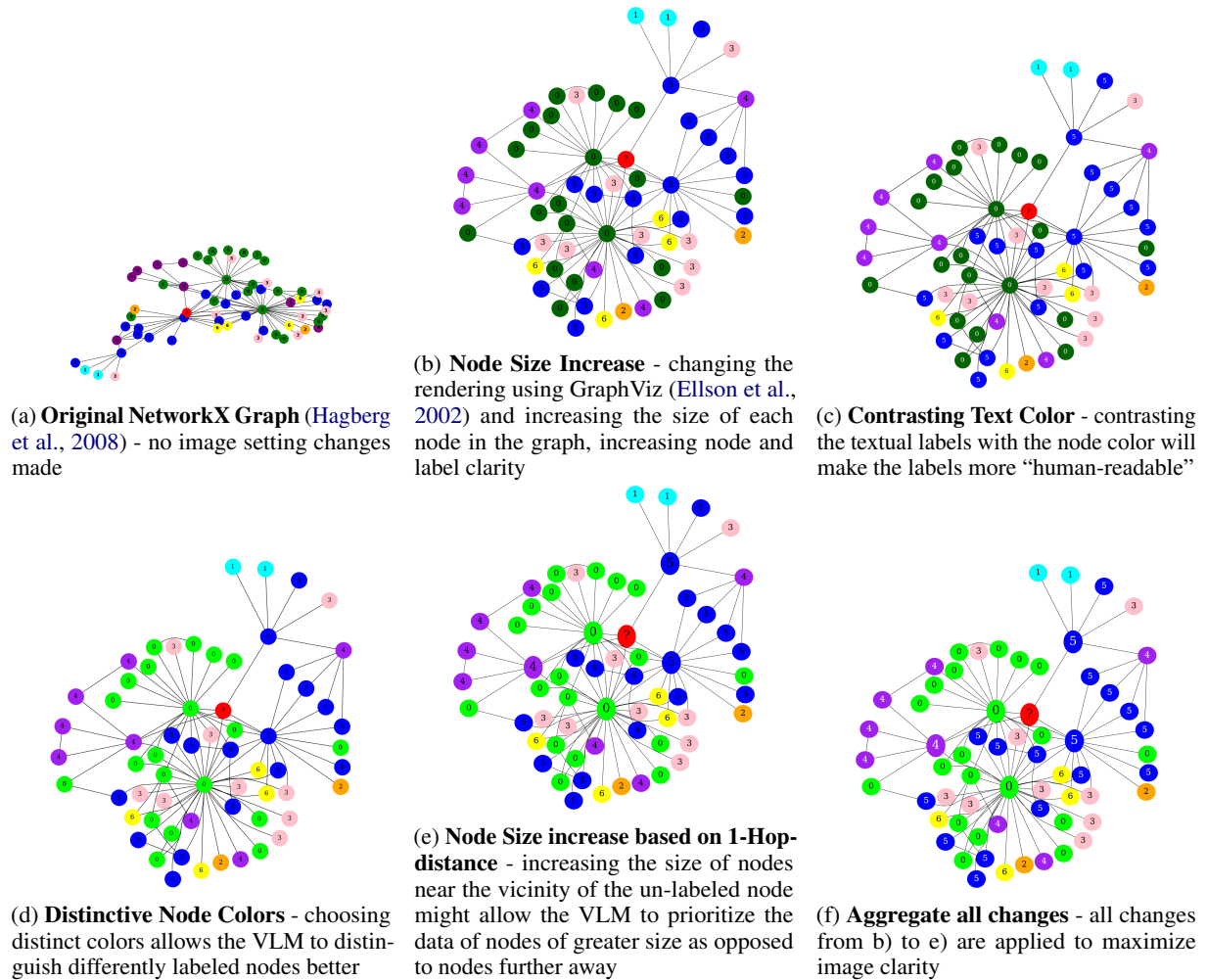


Figure 3: Image representation changes were applied sequentially on a graph, and we observed a distinct **increase from (a) to (f) in human readability and understanding of the graph structure.**

(Graph Text-Motif-Image), a novel benchmark dataset of input graph structures paired with their associated modality encodings (text, motif, and image), associated prompts and resulting LLM classifications. This benchmark will further the community’s understanding of distinct graphs on LLM prompting.

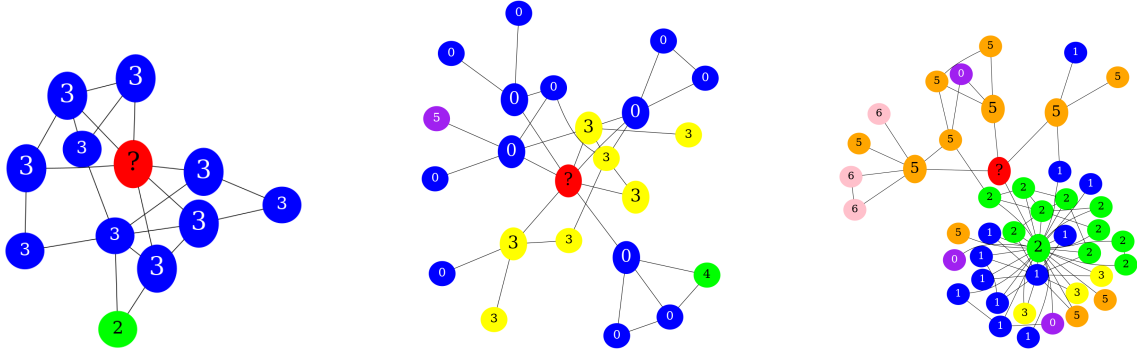
4 Results

4.1 Results Across All Modalities

Comparing Node Classification Performance across Encoding Modalities: Figure 5 shows the node classification performance using the accuracy rate(\uparrow), mismatch rate (\downarrow), denial rate (\downarrow), and token limit fraction (\downarrow) across all encoding modalities. The desired trend is shown in brackets. If we consider only accuracy, we see that the text modality surpasses other modalities but on considering other metrics like denial rate and token limit fraction,

the limitations of the text modality become clear. We observe that the text modality shows a high accuracy rate and token limit fraction. This aligns with this modality’s tendency to provide specific yet verbose local information. We also see a high denial rate with the text modality, and this could be because the long input confuses the LLM, leading it to predict -1 . We observe the benefits associated with the image modality, where it is quite comparable in accuracy rate while having a much lower denial rate and token limit fraction. This shows that the global context provided by the image modality reduces denial by the LLM and requires a much lesser fraction of the context window. Hence, the image modality shows signs of being an informative yet compressive modality.

Comparing Node Classification Accuracies between Graph baselines and LLM models : Table 4 compares the node classification accuracy rates between graph and LLM baselines to see if the



(a) **EASY** - ($\#$ distinct labels < 3) and ($\#$ motifs ≤ 10) (b) **MEDIUM** - ($3 \leq \#$ distinct labels < 5) and ($10 < \#$ motifs ≤ 20) (c) **HARD** - ($\#$ distinct labels ≥ 5) and ($\#$ motifs ≥ 20)

Figure 4: Classifying graph task difficulty based on the criteria of Homophily and Number of Motifs yields a dataset of EASY, MEDIUM, and HARD graph problems and their associated modality encodings and classifications. This benchmark is called the GRAPH-TMI dataset.

| | Model | Cora | Citeseer | Pubmed |
|--------------------------------|-----------|--|--|---|
| GNN
Baselines | GCN | 0.7584 \pm 0.121 | 0.6102 \pm 0.087 | 0.7546 \pm 0.076 |
| | GAT | <u>0.7989</u> \pm 0.092 | 0.6583 \pm 0.074 | 0.7490 \pm 0.060 |
| | GraphSage | 0.7719 \pm 0.124 | 0.6017 \pm 0.103 | 0.7193 \pm 0.076 |
| LLMs +
Encoding
Modality | Text | 0.81 \pm 0.04 [0.07 \pm 0.03] | 0.75 \pm 0.05 [0.07 \pm 0.01] | 0.83 \pm 0.01 [0.08 \pm 0.01]* |
| | Motif | 0.73 \pm 0.06 [0.06 \pm 0.01] | 0.59 \pm 0.01 [0.32 \pm 0.02] | 0.77 \pm 0.006 [0.13 \pm 0.04] |
| | Image | 0.77 \pm 0.05 [0.04 \pm 0.02]* | <u>0.71</u> \pm 0.09 [0.06 \pm 0.0]* | <u>0.79</u> \pm 0.03 [0.19 \pm 0.01] |

Table 4: We report test accuracy rates of node classification across different datasets and denial rates D in [brackets] for LLM models. * indicates the lowest denial rate for each modality. The highest accuracy rate for the dataset is in bold, while the second highest is underlined.

LLM baselines are comparable to the traditional graph methods for node classification across all datasets. We consider a test sample of 50 ego graphs for this apple-to-apple analysis because GPT-V has only released a preview version with a rate limit of 100 RPD (requests per day), which constrains us from extending our analysis to a larger sample. Appendix A shows the test accuracy of the graph baselines with 1000 samples.

From this table, we find that the text modality is comparable with graph baselines in all three datasets, while the image modality comes a close second. This shows the potential of LLMs to be a good foundational model for graphs. We also observe that the lowest denial rate is for the image modality in the smaller CORA and Citeseer datasets, while the bigger Pubmed dataset shows a higher denial rate. This could be because of bigger subgraphs sampled, leading to congestion in the image modality, causing the LLM to deny a classification.

Qualitative analysis of denial of classification

in the Image Modality In Figure 6, we give some examples of graphs sampled from multiple datasets for which GPT-4V denied providing a label (returned -1) using the image modality and the reasons provided by the LLM for denial. We observe that a) the LLM requires context about how labels are assigned to each node. We left this information implicit in our image modality encoder, where every node is colored per its label. The red color is reserved for the ? node, which is unlabeled. This information is not explicit to the LLM. With image (b), there is no clear pattern associating the node’s color with its label, which is a confusion induced by the great amount of heterophily in the graph. Image (c) brings up the need for few-shot learning, where the LLM understands how to infer red nodes given other graph examples.

Insights from GraphTMI We evaluate the accuracy of node classification across multiple modalities, considering the different categories of task

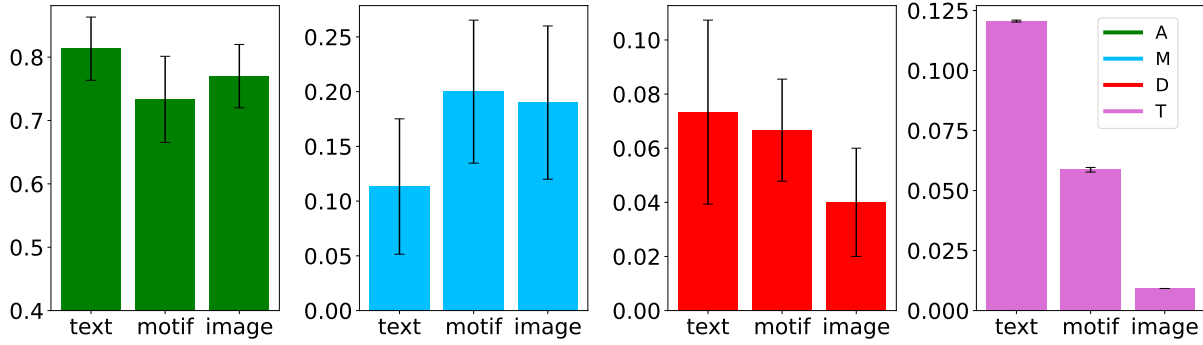


Figure 5: We compare the Modality type (x-axis) with the value of the mean metrics (y-axis). The desired trend is given in brackets for each metric. We observe the accuracy rate (A \uparrow) is comparable between text and image modalities. The motif modality shows the highest mismatch rate (M \downarrow). The image modality shows the least denial rate (D \downarrow). The image modality also shows the least token limit fraction (T \downarrow).

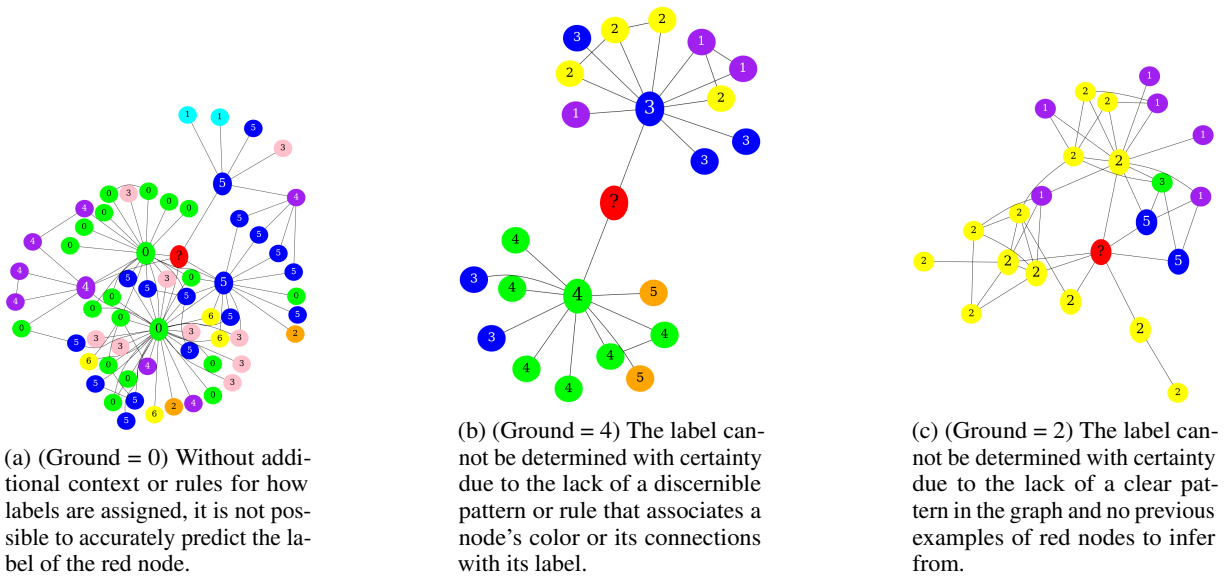


Figure 6: Examples of graphs where VLM (GPT-4V) returned -1 or denied to predict a label and the reason for denial. The ground truth for this graph is given in brackets.

difficulty from the GRAPHTMI benchmark. We observe in Figure 7 that *easy* problems (high homophily, simple graph structure) have higher accuracy with the image modality encoding. Graphs categorized as *medium* or *hard*, because of a heterophyllous nature or complex graph structure, have a higher accuracy with the text modality, though the image modality is not far behind. This is probably because of precise local information provided by the text modality, which is lost in the image modality. This figure illustrates the burgeoning potential of the image modality encoder to solve graph reasoning tasks like node classification with improved representation.

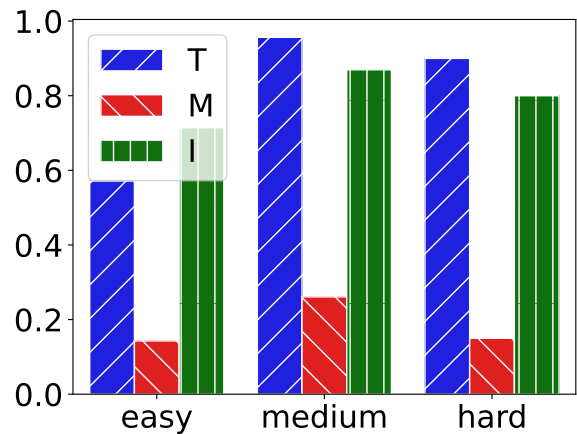


Figure 7: Modality encoder trends with graph task difficulty based on Homophily and Number of Motifs on CORA dataset

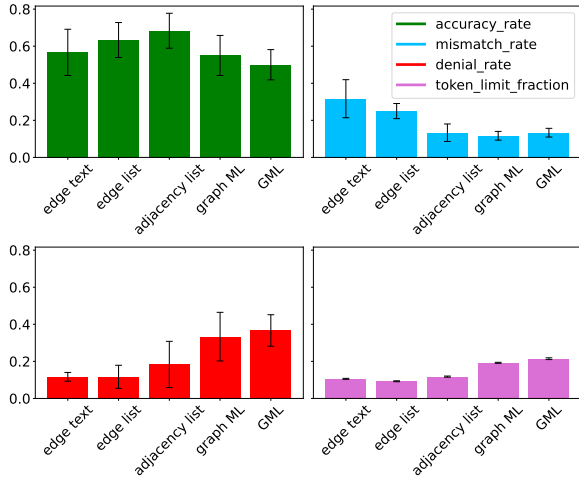


Figure 8: We compare the edge representation type (x-axis) with the value of the mean metrics (y-axis). The desired trend is given in brackets for each metric. The highest performing edge representation is the “adjacency list” representation with the highest accuracy (A ↑) and low mismatch rate (M ↓), denial rate (D ↓), and token limit fraction (T ↓).

4.2 Modality Specific Results

These observations suggest that the choice of dataset and modality can significantly impact the performance metrics

4.2.1 Text Modality Results

Impact of edge encoding function: Figure 8 shows that using the Adjacency List as the mode of edge representation with node label mapping is the most informative encoding function, which balances the trade-off between high accuracy and low token limit fraction.

Impact of graph structure and graph sampling: In Figure 9, we observe the variation of metrics with a chosen dataset (each having a different graph structure) and sampling strategies. CORA displays similarly high accuracy with both sampling techniques, probably because it is the smallest, most dense, most clustered graph. Thus, both sampling strategies would work well with CORA. The denial rate in CORA is lower with ff sampling than ego sampling. Citeseer exhibits the highest denial rate with forest fire (ff) sampling, probably because the local clustering nature is lost in this kind of sampling, leading to an inconsistent sample. It also exhibits the lowest mean accuracy, indicating more challenges in correctly predicting outcomes than the other datasets. Pubmed is the largest dataset, with high connectivity and 1 single component. Therefore, the samples generated via

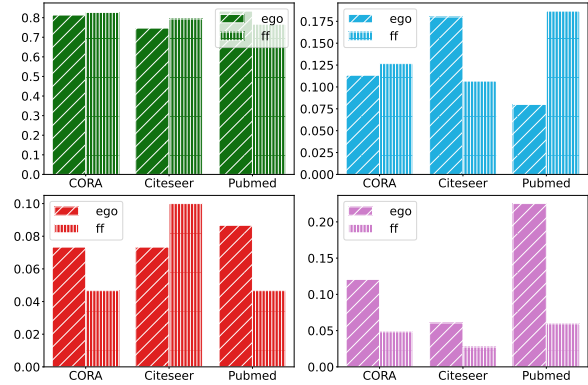


Figure 9: We compare the mean metrics (y-axis) for each dataset and sampling type (x-axis). Green is the accuracy rate, Blue is the mismatch rate, Red is the denial rate, and Pink is the token limit fraction. The desired trends for each metric are given in brackets - (↑) accuracy rate, (↓) mismatch rate, (↓) denial rate, and (↓) token limit fraction. The x-axis distinguishes between ego graph sampling (ego) and forest fire sampling (ff) through different bar textures.

ego graph sampling with Pubmed generally tend to be large - leading to an increased token limit fraction. Citeseer, on the other hand, is a fragmented, disconnected dataset with more local connectivity. Therefore, ego graph samples from Citeseer are smaller and have a lower token limit fraction.

4.2.2 Motif Modality Results

Figure 10 illustrates the performance of GPT-4 on introducing different motif information changes as a part of the motif modality encoder. Table 3 explains the intuition behind these changes. We observe that the mean accuracy rate goes up on adding the “triangle and star attached to ? node” motif, while the other metrics for the same setting are low. The higher performance of this motif information is likely because of the local and global context given to the LLM through the node-label mapping and the actual nodes associated with each other as part of triads or star motifs.

4.2.3 Image Modality Results

Figure 8 describes how we introduce multiple changes to represent an image, and Figure 11 illustrates that the best setting can be determined by looking at the highest mean accuracy, low mean denial rate, and mismatch rate of the node classification. We observe that the “rendering change” offers the highest bump in accuracy, which only goes down when “node size is changed on hop”. This is probably because the LLM is confused by

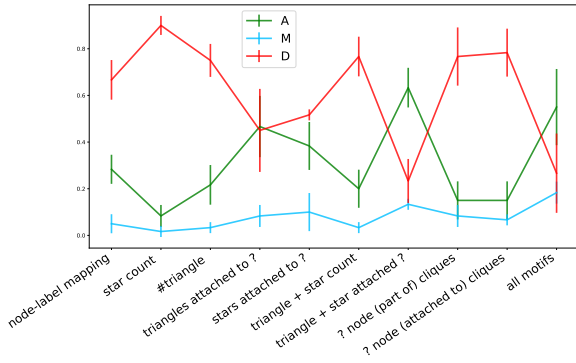


Figure 10: We compare the motif information (x-axis) to the mean metrics (y-axis). Desired trends are denoted in brackets. Metrics considered are Accuracy Rate (A \uparrow), Mismatch Rate (M \downarrow), and Denial Rate (D \downarrow). The highest performing motif information change “triangle and star attached to ?” has higher accuracy and lower mismatch and denial rate.

different node sizes and their meaning. This could be resolved by clarifying the text prompt or using different shapes to represent nodes at different hop distances. Based on Figure 11, when “all the changes are applied”, the denial rate is minimum, and the accuracy rate is highest (0.7).

5 Related Work

GNN-based methods GNNs are particularly effective for node classification and link prediction (Dwivedi et al., 2020), with applications across social networks, computer vision, chemistry, and biology (Hou et al., 2022). Their reliance on complete network structures, often unavailable in real-world settings (Wei and Hu, 2022), is mitigated through graph sampling techniques (Ahmed et al., 2013). Prominent GNN models include Graph Convolutional Networks (GCN) (Kipf and Welling, 2016), GraphSage (Hamilton et al., 2017), and Graph Attention Networks (GAT) (Veličković et al., 2017), each having unique features and applications. A significant limitation of GNNs is their inability to process non-numeric data directly, like text and images, which requires preprocessing steps like feature engineering (Wang et al., 2021).

LLMs for graph reasoning Recent research has delved into using Large Language Models (LLMs) for tasks involving implicit graphical structures, revealing their potential in various complex reasoning domains (Huang et al., 2022). Integrating LLMs with graph-based tasks have been explored by (He et al., 2023), where LLM explanations are

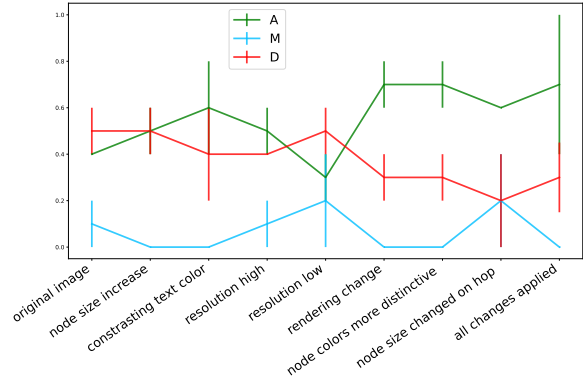


Figure 11: We compare the image representations (x-axis) to the mean metrics (y-axis). Desired trends are denoted in brackets. Metrics considered are Accuracy Rate (A \uparrow), Mismatch Rate (M \downarrow), and Denial Rate (D \downarrow). The highest performing image representation “all changes applied” has a higher accuracy and lower mismatch rate

used to train Message Passing Neural Networks (MPNNs) in node category prediction. (Chen et al., 2023) expanded the use of LLMs to enhance features and predict node classifications. (Wang et al., 2023) introduced NLGraph, a benchmark for evaluating LLMs in traditional graph tasks. Additionally, (Guo et al., 2023) conducted an empirical study on LLMs’ abilities in tasks requiring structural and semantic understanding. All these studies use LLMs as a sub-component, such as a feature extractor, within conventional graph learning frameworks.

Prompt Design for Graphs Different prompting approaches for querying large language models (LLMs) primarily focus on optimizing the prompt’s text to improve task performance. Zero-shot prompting presents the model with only a task description, relying on the model’s pre-existing knowledge to generate the correct output. Few-shot in-context learning (Brown et al., 2020) goes a step further by providing a few examples of the task with the desired outputs, which the model then uses to learn and apply to new inputs. Chain-of-thought prompting (Wei et al., 2022) gives the model step-by-step examples detailing the problem-solving process, encouraging it to generate its reasoning paths. A variant of this, zero-shot CoT (Kojima et al., 2022), skips prior examples and prompts the model to produce its reasoning chains with a simple starter phrase. Bag prompting (Wang et al., 2023) is tailored for graph-related tasks, suggesting the construction of a graph before attempting the task. (Guo et al., 2023) propose methods like

format explanations and role prompting for clearer task understanding and strategic input arrangement to exploit LLMs' in-context learning. Additionally, they highlight self-prompting, where the LLM refines prompts through context summarization, addressing the challenges of inadequate or overly complex graph information.

6 Future Work

Future research based on this study can advance in several directions. A crucial development would be integrating multiple modalities for node classification, enhancing accuracy, and providing comprehensive insights into node characteristics across varying graph structures. Another promising avenue is applying these findings to text-attributed graphs. This approach, focusing on encoding rich textual node and behavioral information, can deepen the understanding of complex networks.

Exploring heterogeneous graphs, which feature diverse node and edge types unlike the homogenous graphs studied here, is another key area. Applying different modalities, especially image modality, to represent the varied entities in these graphs, prevalent in real-world applications like social networks, can offer significant advancements.

Broadening the study to encompass other semantic graph reasoning tasks, including link prediction, community detection, and graph classification, can also extend its practical applicability. These tasks are essential for a comprehensive grasp of complex network structures.

Lastly, applying these methodologies to directed graphs, which have unique characteristics and challenges distinct from undirected graphs, represents a valuable research opportunity. Tailoring and refining the study's approaches for directed graphs could provide critical insights and practical applications across various domains.

7 Conclusion

This research delves into the application of Large Language Models (LLMs) in tasks involving graph-structured data, a crucial step towards artificial general intelligence (AGI). While LLMs have shown versatility in domains like social network analysis, drug discovery, and recommendation systems, they face challenges due to their reliance on unstructured text, leading to issues like hallucination and logical oversights. This paper proposes addressing these limitations through graph-structured data,

exploring efficient input encoding modalities, and prompt designing for graph tasks.

The study focuses on graph node classification, evaluating the effectiveness of different encoding modalities - text, image, and motif - for LLMs. It introduces innovative approaches like motif modality encoding, which balances local and global perspectives, and image modality encoding, which leverages vision-capable LLMs like GPT-4V for a more global view with efficient token usage. Key contributions of this research include a comprehensive analysis of graph-structure prompting in various modalities and the introduction of the GRAPHTMI benchmark. The findings indicate that image modality is more effective than text for balancing token limits and retaining essential information. The study also highlights how graph task difficulty, edge encoding functions, graph structure, graph sampling techniques, and motif information impact node classification performance.

The empirical results reveal that while LLMs are improving in handling graph data, they lag behind Graph Neural Network (GNN) models in real-world graph applications. This study identifies current limitations and potential future directions for LLMs, particularly in understanding graphs and performing reasoning tasks with image capabilities.

Limitations

Although innovative in applying Large Language Models (LLMs) to graph-structured data, this research faces key limitations. The computational demands of detecting network motifs, essential for understanding complex network dynamics, pose a significant challenge. This process requires extensive computational power and advanced algorithms, limiting scalability and efficiency. We subvert these challenges by restricting our subgraph sample size to 3 hops of an ego graph. Additionally, the study is constrained by the current rate limitations of GPT-V, which affects its ability to process and analyze data at scale efficiently. This limitation restricts the depth and scope of the analysis, although future advancements in GPT-V may mitigate this issue. A further limitation lies in the study's simplistic approach to estimating homophily, relying merely on label count and neglecting the importance of hop distance. This overlooks critical network structure and node similarity aspects, leading to a potentially oversimplified analysis. Incorporating hop distance

could provide a more accurate representation of network homophily. These limitations underscore the need for further advancements in computational techniques, model capabilities, and more nuanced theoretical methods in network analysis.

Acknowledgements

We thank the members of the MinnesotaNLP research group for their feedback on our project and fruitful discussion. This was instrumental to our project and helped us clarify our research.

References

- Nesreen K Ahmed, Jennifer Neville, and Ramana Kompella. 2013. Network sampling: From static to streaming graphs. *ACM Transactions on Knowledge Discovery from Data (TKDD)*, 8(2):1–56.
- Jacob Andreas. 2022. Language models as agent models. *arXiv preprint arXiv:2212.01681*.
- Tom Brown, Benjamin Mann, Nick Ryder, Melanie Subbiah, Jared D Kaplan, Prafulla Dhariwal, Arvind Neelakantan, Pranav Shyam, Girish Sastry, Amanda Askell, et al. 2020. Language models are few-shot learners. *Advances in neural information processing systems*, 33:1877–1901.
- Sébastien Bubeck, Varun Chandrasekaran, Ronen Eldan, Johannes Gehrke, Eric Horvitz, Ece Kamar, Peter Lee, Yin Tat Lee, Yuanzhi Li, Scott Lundberg, et al. 2023. Sparks of artificial general intelligence: Early experiments with gpt-4. *arXiv preprint arXiv:2303.12712*.
- Peter J Carrington, John Scott, and Stanley Wasserman. 2005. *Models and methods in social network analysis*, volume 28. Cambridge university press.
- Zhikai Chen, Haitao Mao, Hang Li, Wei Jin, Hongzhi Wen, Xiaochi Wei, Shuaiqiang Wang, Dawei Yin, Wenqi Fan, Hui Liu, et al. 2023. Exploring the potential of large language models (llms) in learning on graphs. *arXiv preprint arXiv:2307.03393*.
- Vijay Prakash Dwivedi, Chaitanya K Joshi, Anh Tuan Luu, Thomas Laurent, Yoshua Bengio, and Xavier Bresson. 2020. Benchmarking graph neural networks. *arXiv preprint arXiv:2003.00982*.
- John Ellson, Emden Gansner, Lefteris Koutsofios, Stephen C North, and Gordon Woodhull. 2002. Graphviz—open source graph drawing tools. In *Graph Drawing: 9th International Symposium, GD 2001 Vienna, Austria, September 23–26, 2001 Revised Papers 9*, pages 483–484. Springer.
- Bahare Fatemi, Jonathan Halcrow, and Bryan Perozzi. 2023. Talk like a graph: Encoding graphs for large language models. *arXiv preprint arXiv:2310.04560*.
- Diane Felmlee, Cassie McMillan, and Roger Whitaker. 2021. Dyads, triads, and tetrads: a multivariate simulation approach to uncovering network motifs in social graphs. *Applied network science*, 6(1):1–26.
- C Lee Giles, Kurt D Bollacker, and Steve Lawrence. 1998. Citeseer: An automatic citation indexing system. In *Proceedings of the third ACM conference on Digital libraries*, pages 89–98.
- Jiayan Guo, Lun Du, and Hengyu Liu. 2023. Gpt4graph: Can large language models understand graph structured data? an empirical evaluation and benchmarking. *arXiv preprint arXiv:2305.15066*.
- Aric Hagberg, Pieter Swart, and Daniel S Chult. 2008. Exploring network structure, dynamics, and function using networkx. Technical report, Los Alamos National Lab.(LANL), Los Alamos, NM (United States).
- Will Hamilton, Zhitao Ying, and Jure Leskovec. 2017. Inductive representation learning on large graphs. *Advances in neural information processing systems*, 30.
- Xiaoxin He, Xavier Bresson, Thomas Laurent, and Bryan Hooi. 2023. Explanations as features: Llm-based features for text-attributed graphs. *arXiv preprint arXiv:2305.19523*.
- Paul W Holland and Samuel Leinhardt. 1974. The statistical analysis of local structure in social networks.
- Yifan Hou, Jian Zhang, James Cheng, Kaili Ma, Richard TB Ma, Hongzhi Chen, and Ming-Chang Yang. 2022. Measuring and improving the use of graph information in graph neural networks. *arXiv preprint arXiv:2206.13170*.
- Jie Huang and Kevin Chen-Chuan Chang. 2022. Towards reasoning in large language models: A survey. *arXiv preprint arXiv:2212.10403*.
- Wenlong Huang, Pieter Abbeel, Deepak Pathak, and Igor Mordatch. 2022. Language models as zero-shot planners: Extracting actionable knowledge for embodied agents. In *International Conference on Machine Learning*, pages 9118–9147. PMLR.
- Thomas N Kipf and Max Welling. 2016. Semi-supervised classification with graph convolutional networks. *arXiv preprint arXiv:1609.02907*.
- Takeshi Kojima, Shixiang Shane Gu, Machel Reid, Yutaka Matsuo, and Yusuke Iwasawa. 2022. Large language models are zero-shot reasoners. *Advances in neural information processing systems*, 35:22199–22213.
- Jure Leskovec and Christos Faloutsos. 2006. Sampling from large graphs. In *Proceedings of the 12th ACM SIGKDD international conference on Knowledge discovery and data mining*, pages 631–636.

- Patrick Lewis, Ethan Perez, Aleksandra Piktus, Fabio Petroni, Vladimir Karpukhin, Naman Goyal, Heinrich Küttler, Mike Lewis, Wen-tau Yih, Tim Rocktäschel, et al. 2020. Retrieval-augmented generation for knowledge-intensive nlp tasks. *Advances in Neural Information Processing Systems*, 33:9459–9474.
- Aman Madaan, Shuyan Zhou, Uri Alon, Yiming Yang, and Graham Neubig. 2022. Language models of code are few-shot commonsense learners. *arXiv preprint arXiv:2210.07128*.
- Andrew Kachites McCallum, Kamal Nigam, Jason Renzie, and Kristie Seymore. 2000. Automating the construction of internet portals with machine learning. *Information Retrieval*, 3:127–163.
- Miller McPherson, Lynn Smith-Lovin, and James M Cook. 2001. Birds of a feather: Homophily in social networks. *Annual review of sociology*, 27(1):415–444.
- Prem Melville and Vikas Sindhwani. 2010. Recommender systems. *Encyclopedia of machine learning*, 1:829–838.
- Ron Milo, Shai Shen-Orr, Shalev Itzkovitz, Nadav Keshatan, Dmitri Chklovskii, and Uri Alon. 2002. Network motifs: simple building blocks of complex networks. *Science*, 298(5594):824–827.
- Alan Mislove, Massimiliano Marcon, Krishna P Gummadi, Peter Druschel, and Bobby Bhattacharjee. 2007. Measurement and analysis of online social networks. In *Proceedings of the 7th ACM SIGCOMM conference on Internet measurement*, pages 29–42.
- OpenAI. 2023a. Gpt-4 system card. <https://openai.com/research/gpt-4v-system-card>.
- OpenAI. 2023b. Gpt-4v(ision) system card. https://cdn.openai.com/papers/GPTV_System_Card.pdf.
- John Palowitch, Anton Tsitsulin, Brandon Mayer, and Bryan Perozzi. 2022. Graphworld: Fake graphs bring real insights for gnns. In *Proceedings of the 28th ACM SIGKDD Conference on Knowledge Discovery and Data Mining*, pages 3691–3701.
- Shirui Pan, Linhao Luo, Yufei Wang, Chen Chen, Jipu Wang, and Xindong Wu. 2023. Unifying large language models and knowledge graphs: A roadmap. *arXiv preprint arXiv:2306.08302*.
- Prithviraj Sen, Galileo Namata, Mustafa Bilgic, Lise Getoor, Brian Galligher, and Tina Eliassi-Rad. 2008. Collective classification in network data. *AI magazine*, 29(3):93–93.
- Simon Stolz and Christian Schlereth. 2021. Predicting tie strength with ego network structures. *Journal of Interactive Marketing*, 54(1):40–52.
- Kun Tu, Jian Li, Don Towsley, Dave Braines, and Liam D Turner. 2018. Network classification in temporal networks using motifs. *arXiv preprint arXiv:1807.03733*.
- Petar Veličković, Guillem Cucurull, Arantxa Casanova, Adriana Romero, Pietro Lio, and Yoshua Bengio. 2017. Graph attention networks. *arXiv preprint arXiv:1710.10903*.
- Saraswathi Vishveshwara, KV Brinda, and Natarajan Kannan. 2002. Protein structure: insights from graph theory. *Journal of Theoretical and Computational Chemistry*, 1(01):187–211.
- Heng Wang, Shangbin Feng, Tianxing He, Zhaoxuan Tan, Xiaochuang Han, and Yulia Tsvetkov. 2023. Can language models solve graph problems in natural language? *arXiv preprint arXiv:2305.10037*.
- Yangkun Wang, Jiarui Jin, Weinan Zhang, Yong Yu, Zheng Zhang, and David Wipf. 2021. Bag of tricks for node classification with graph neural networks. *arXiv preprint arXiv:2103.13355*.
- Jason Wei, Xuezhi Wang, Dale Schuurmans, Maarten Bosma, Fei Xia, Ed Chi, Quoc V Le, Denny Zhou, et al. 2022. Chain-of-thought prompting elicits reasoning in large language models. *Advances in Neural Information Processing Systems*, 35:24824–24837.
- Qiang Wei and Guangmin Hu. 2022. Evaluating graph neural networks under graph sampling scenarios. *PeerJ Computer Science*, 8:e901.
- Carl Yang, Mengxiong Liu, Vincent W Zheng, and Jiawei Han. 2018. Node, motif and subgraph: Leveraging network functional blocks through structural convolution. in 2018 IEEE. In *ACM International Conference on Advances in Social Networks Analysis and Mining (ASONAM)*, pages 47–52.
- Mustafa Yasir, John Palowitch, Anton Tsitsulin, Long Tran-Thanh, and Bryan Perozzi. 2023. Examining the effects of degree distribution and homophily in graph learning models. *arXiv preprint arXiv:2307.08881*.
- Shukang Yin, Chaoyou Fu, Sirui Zhao, Ke Li, Xing Sun, Tong Xu, and Enhong Chen. 2023. A survey on multimodal large language models. *arXiv preprint arXiv:2306.13549*.
- Yue Zhang, Yafu Li, Leyang Cui, Deng Cai, Lemao Liu, Tingchen Fu, Xinting Huang, Enbo Zhao, Yu Zhang, Yulong Chen, et al. 2023. Siren’s song in the ai ocean: A survey on hallucination in large language models. *arXiv preprint arXiv:2309.01219*.

A Training Details for GNN models

For training our GNN models, we used the following hyperparameters. The training and test set

Table 5: Graph Properties and Their Descriptions

| Name of Property | Description |
|------------------------|--|
| Density | Measures how connected the graph is. It’s the ratio of actual edges to possible edges. |
| Degree Distribution | The distribution of node degrees. The histogram might follow a specific pattern (e.g., power-law distribution, Gaussian distribution). |
| Average Degree | The average degree of nodes in the graph. |
| Connected Components | A subgraph in which a path connects any two nodes. |
| Clustering Coefficient | Measures the degree to which nodes tend to cluster together. |
| Graph Diameter | The longest shortest path between any two nodes. It provides insight into the graph’s overall size. |
| 2hop nodes | Average number of nodes present in the subgraph at 2 hop distance from any node |

| | Model | Cora | Citeseer | Pubmed |
|------------------|-----------|--|--|---|
| GNN
Baselines | GCN | 0.7820 \pm 0.133 | 0.6540 \pm 0.083 | 0.7480 \pm 0.077 |
| | GAT | 0.8200 \pm 0.084 | 0.6680 \pm 0.069 | 0.7510 \pm 0.050 |
| | GraphSage | 0.7570 \pm 0.137 | 0.6300 \pm 0.098 | 0.7430 \pm 0.078 |
| LLMs + | Text | <u>0.81</u> \pm 0.04 [0.07 \pm 0.03] | 0.75 \pm 0.05 [0.07 \pm 0.01] | 0.83 \pm 0.01 [0.08 \pm 0.01]* |
| Encoding | Motif | 0.73 \pm 0.06 [0.06 \pm 0.01] | 0.59 \pm 0.01 [0.32 \pm 0.02] | 0.77 \pm 0.006 [0.13 \pm 0.04] |
| Modality | Image | 0.77 \pm 0.05 [0.04 \pm 0.02]* | <u>0.71</u> \pm 0.09 [0.06 \pm 0.0]* | <u>0.79</u> \pm 0.03 [0.19 \pm 0.01] |

Table 6: Test accuracy rates of node classification across different datasets using the entire 1000 test data and denial rates D in [brackets] for LLM models. For LLMs, we chose a test sample of 50 graphs. * indicates the lowest denial rate for each modality. The highest accuracy rate for the dataset is in bold, while the second highest is underlined.

details are given below. We also report the parameters of each model. In the main paper, report the GNN test accuracy on 50 samples due to API constraints by GPT-4, which do not allow us to conduct the apple-to-apple comparison with 1000 test samples. However, Table 6 reports the test accuracy for GNN reported on 1000 samples.

B Specifics of LLM Experiments

Token limits for each modality Due to their architecture, transformer-based models like GPT-3 and GPT-4 have a fixed-size attention window. This determines how many tokens the model can “remember” or pay attention to at once. This limit also manages the computational cost of running the model and the model’s performance. The token limit constraint for GPT-4 is 8192 tokens, while for GPT-4V(vision), the limit is claimed to be 128000 tokens, but currently, only the preview version has been released, and the actual limit is 10000 tokens.

Rate limits for each LLM For a tier 5 user, the rate

limit for GPT-4 is 10K RPM (requests per minute), and for GPT-4V, the rate limit is 100 RPD (requests per day).

Modality Experiments For text and motif type, we sample 20 graphs, number of hops considered = 3, no of runs = 3, and perform ego graph and forest fire sampling. In the paper, we report the results from ego graph sampling because node classification typically needs a Localized View Around Specific Nodes, best provided by ego graph sampling. With Image Modality Experiments, we sample 50 ego-graphs and no of runs = 2, as rate limitations constrain us.

Graph Structure Properties Table 5 provides definitions for network properties. The average number of nodes and edges in a 2-hop subgraph is also reported for CORA, Citeseer and Pubmed datasets.

| | CORA | Citeseer | Pubmed |
|-----------------------------------|-------------------|-------------------|---------------------|
| Avg no of edges in 2 hop subgraph | 62.70 \pm 94.77 | 26.35 \pm 61.70 | 129.36 \pm 287.61 |
| Avg no of nodes in 2 hop subgraph | 36.78 \pm 48.12 | 15.11 \pm 24.73 | 60.05 \pm 85.12 |

Table 7: Subgraph Sampling Stats

| Details | GCN | GAT | GraphSAGE |
|----------------|------------|------------|------------------|
| Epochs | 100 | 100 | 100 |
| Learning Rate | 0.005 | 0.005 | 0.005 |
| Weight Decay | 5e-4 | 5e-4 | 5e-4 |

Table 8: List of GNN training hyperparameters

| Dataset | Cora | Citeseer | Pubmed |
|------------------|-------------|-----------------|---------------|
| Training Set | 140 | 120 | 60 |
| Testing Set | 1000 | 1000 | 1000 |
| GCN Parameters | 23063 | 59366 | 8067 |
| GAT Parameters | 92373 | 237586 | 32393 |
| GraphSage Params | 46103 | 118710 | 16115 |

Table 9: GNN Training/Testing and Parameters per dataset